


Back-reaction and correlation effects on prethermalization in Mott-Hubbard systems

Friedemann Queisser¹,[✉] Christian Kohlfürst¹,[✉] and Ralf Schützhold^{1,2}

¹*Helmholtz-Zentrum Dresden-Rossendorf, Bautzner Landstraße 400, 01328 Dresden, Germany*

²*Institut für Theoretische Physik, Technische Universität Dresden, 01062 Dresden, Germany*

 (Received 21 November 2023; revised 15 April 2024; accepted 22 April 2024; published 13 May 2024)

For the Fermi-Hubbard model in the strongly interacting Mott insulator state, we study the prethermalization dynamics after a quench (switching on the hopping rate). To this end, we employ the method of the hierarchy of correlations and compare different levels of accuracy. To leading order, the usual free quasiparticle dynamics (as encoded in the two-point correlation functions) yields the standard picture of prethermalization. Taking into account the back-reaction of these quasiparticle fluctuations onto the mean-field background as the first next-to-leading-order effect, we observe a strong degradation of prethermalization, especially in low dimensions. In contrast, the inclusion of three-point correlations enhances prethermalization.

DOI: [10.1103/PhysRevB.109.195140](https://doi.org/10.1103/PhysRevB.109.195140)

I. INTRODUCTION

The question of how quantum many-body systems relax back to thermal equilibrium after being excited by an external stimulus has been the topic of active research [1–47] and is still not completely understood, especially for strongly interacting systems. As an indicator of the complexity of this problem, this relaxation dynamics can occur in various stages and on different timescales.

To be more specific, let us consider a global stimulus in the form of a quench by suddenly (or rapidly) changing one or more parameters of the system, which drives it out of equilibrium. In a quasiparticle picture, this departure from equilibrium can be understood as the excitation of many quasiparticle modes. Moreover, such a quench typically corresponds to a coherent stimulus (rather than an incoherent, e.g., thermal, excitation) such that these quasiparticle modes all have the same phase, at least initially. As a result of this coherence, local quantities typically start oscillating after the quench as the phases of the quasiparticle modes evolve with time. However, due to the distribution or dispersion of the quasiparticle energies, their phases evolve differently and thus get scrambled. As a result, the fluctuations of local quantities diminish gradually, approaching quasistationary values as time progresses.

Note, however, that this quasistationary state is not necessarily the thermal equilibrium state—only the phases of the quasiparticle modes have become scrambled; their distribution has not changed yet and generally differs from a thermal distribution [48,49]. Thus, this initial stage of dephasing is usually referred to as prethermalization; full thermalization would also require the approach to thermal distribution functions, which can be achieved via Boltzmann collision dynamics (and requires interactions between the quasiparticles) [50–54].

This complexity of the relaxation dynamics is already present for weakly interacting systems, but it can become even more challenging for strongly interacting quantum many-body systems. In the following, we study the prethermalization dynamics in the Mott insulator state of the

Fermi-Hubbard model. We place special emphasis on the impact of back-reaction and higher-order correlations in order to understand how these effects might change the usual picture. In order to base our investigations on a well-defined analytical expansion in terms of a control parameter, we employ the method of the hierarchy of correlations [55].

II. FERMIONIC HUBBARD MODEL

To analyze the prethermalization dynamics of a prototypical strongly interacting quantum many-body system, we consider the fermionic Hubbard model. The Hamiltonian governing the system is given by ($\hbar = 1$)

$$\hat{H} = -\frac{1}{Z} \sum_{\mu\nu s} T_{\mu\nu} \hat{c}_{\mu s}^\dagger \hat{c}_{\nu s} + U \sum_{\mu} \hat{n}_{\mu}^\uparrow \hat{n}_{\mu}^\downarrow. \quad (1)$$

The fermionic creation and annihilation operators at sites μ and ν , with spin $s \in \uparrow, \downarrow$, are denoted as $\hat{c}_{\mu s}^\dagger$ and $\hat{c}_{\nu s}$, respectively. The hopping matrix $T_{\mu\nu}(t)$ is only nonvanishing for nearest neighbors where it adopts the value of the tunneling rate $T(t)$, which can depend on time. The coordination number Z represents the number of nearest neighbors for a given lattice site. In the following, we shall consider the scenario in which the system is initially prepared in a stationary state at half filling for $T = 0$. Then the tunneling rate is switched to a finite value $T > 0$. For simplicity, we consider a sudden change $T(t) = T\Theta(t)$, but the analysis can easily be generalized to other scenarios.

A. The hierarchy of correlations

Apart from finite lattices (e.g., the Hubbard dimer), exact solutions of the fermionic Hubbard model (1) are available only in one spatial dimension [56] or in the limit of infinite dimensions [57]. To derive approximate solutions in finite but high dimensions, we employ a hierarchical method suitable for systems with large coordination numbers Z . Hence, we partition the reduced density matrices into correlations between lattice sites and on-site density matrices $\hat{\rho}_{\mu}$. For

instance, the correlation between two sites is defined as $\hat{\rho}_{\mu\nu}^{\text{corr}} = \hat{\rho}_{\mu\nu} - \hat{\rho}_\mu \hat{\rho}_\nu$. Similarly, correlations among three sites can be expressed as $\hat{\rho}_{\mu\nu\lambda}^{\text{corr}} = \hat{\rho}_{\mu\nu\lambda} - \hat{\rho}_\mu \hat{\rho}_\nu \hat{\rho}_\lambda - \hat{\rho}_{\mu\nu}^{\text{corr}} \hat{\rho}_\lambda - \hat{\rho}_{\mu\lambda}^{\text{corr}} \hat{\rho}_\nu - \hat{\rho}_{\nu\lambda}^{\text{corr}} \hat{\rho}_\mu$ and so forth.

The on-site density matrix $\hat{\rho}_\mu$ and the two-site correlators $\hat{\rho}_{\mu\nu}^{\text{corr}}$ follow evolution equations, which can be represented schematically as [55]

$$i\partial_t \hat{\rho}_\mu = F_1(\hat{\rho}_\mu, \hat{\rho}_{\mu\nu}^{\text{corr}}) = O(1), \quad (2)$$

$$i\partial_t \hat{\rho}_{\mu\nu}^{\text{corr}} = F_2(\hat{\rho}_\mu, \hat{\rho}_{\mu\nu}^{\text{corr}}, \hat{\rho}_{\mu\nu\lambda}^{\text{corr}}) = O(1/Z), \quad (3)$$

$$i\partial_t \hat{\rho}_{\mu\nu\lambda}^{\text{corr}} = F_3(\hat{\rho}_\mu, \hat{\rho}_{\mu\nu}^{\text{corr}}, \hat{\rho}_{\mu\nu\lambda}^{\text{corr}}, \hat{\rho}_{\mu\nu\lambda\kappa}^{\text{corr}}) = O(1/Z^2). \quad (4)$$

Similar equations apply to higher-order correlations. The specific forms of the nonlinear functions F_n are determined by the exact von Neumann equation for the density matrix of the Hubbard model (1). Analyzing the evolution equations for the correlators reveals that the scaling hierarchy remains preserved over time when the initial values satisfy $\hat{\rho}_\mu = O(1)$, $\hat{\rho}_{\mu\nu}^{\text{corr}} = O(1/Z)$, and so on [58,59].

Introducing the following operators proves to be advantageous when analyzing the evolution equation:

$$\hat{c}_{\mu s I} = \hat{c}_{\mu s} \hat{n}_{\mu \bar{s}}^I = \begin{cases} \hat{c}_{\mu s} (1 - \hat{n}_{\mu \bar{s}}) & \text{for } I = 0, \\ \hat{c}_{\mu s} \hat{n}_{\mu \bar{s}} & \text{for } I = 1. \end{cases} \quad (5)$$

Here, \bar{s} denotes the opposite spin to s . Intuitively, $\hat{c}_{\mu s I}$ annihilates a fermion with spin s from a doubly occupied lattice site μ for $I = 1$ but creates an empty lattice site μ for $I = 0$ and is thus a precursor for doublon and holon quasiparticle operators.

The site-local quantities follow the evolution equation

$$\begin{aligned} i\partial_t \langle \hat{n}_{\mu s I} \hat{n}_{\mu \bar{s} J} \rangle &= \frac{(-1)^I}{Z} \sum_{\kappa, K} T_{\mu\kappa} [\langle \hat{c}_{\mu s I}^\dagger \hat{c}_{\kappa s K} \rangle^{\text{corr}} - \langle \hat{c}_{\kappa s K}^\dagger \hat{c}_{\mu s I} \rangle^{\text{corr}}] \\ &+ \frac{(-1)^J}{Z} \sum_{\kappa, K} T_{\mu\kappa} [\langle \hat{c}_{\mu \bar{s} J}^\dagger \hat{c}_{\kappa \bar{s} K} \rangle^{\text{corr}} - \langle \hat{c}_{\kappa \bar{s} K}^\dagger \hat{c}_{\mu \bar{s} J} \rangle^{\text{corr}}]. \end{aligned} \quad (6)$$

By definition, the two-site correlators between sites μ and ν are nonzero only for $\mu \neq \nu$. This is expressed formally as $\langle \hat{c}_{\mu s I}^\dagger \hat{c}_{\nu s J} \rangle^{\text{corr}} = \langle \hat{c}_{\mu s I}^\dagger \hat{c}_{\nu s J} \rangle - \delta_{\mu\nu} \delta_{IJ} \langle \hat{n}_{\mu s} \hat{n}_{\mu \bar{s}} \rangle$. The behavior of these two-site correlators is determined by their evolution equation,

$$\begin{aligned} i\partial_t \langle \hat{c}_{\mu s I}^\dagger \hat{c}_{\nu s J} \rangle^{\text{corr}} &= U(J - I) \langle \hat{c}_{\mu s I}^\dagger \hat{c}_{\nu s J} \rangle^{\text{corr}} \\ &+ \sum_{\kappa, K} \frac{T_{\mu\kappa}}{Z} \langle \hat{n}_{\mu \bar{s} I} \rangle \langle \hat{c}_{\kappa s K}^\dagger \hat{c}_{\nu s J} \rangle^{\text{corr}} + \frac{T_{\mu\nu}}{Z} \langle \hat{n}_{\mu \bar{s} I} \rangle \langle \hat{n}_{\nu s 1} \hat{n}_{\nu \bar{s} J} \rangle \\ &- \sum_{\kappa, K} \frac{T_{\nu\kappa}}{Z} \langle \hat{n}_{\nu \bar{s} J} \rangle \langle \hat{c}_{\mu s I}^\dagger \hat{c}_{\kappa s K} \rangle^{\text{corr}} - \frac{T_{\mu\nu}}{Z} \langle \hat{n}_{\nu \bar{s} J} \rangle \langle \hat{n}_{\mu s 1} \hat{n}_{\mu \bar{s} I} \rangle \\ &- \delta_{\mu\nu} \sum_{\kappa, K} \frac{T_{\mu\kappa}}{Z} [\langle \hat{n}_{\mu \bar{s} I} \rangle \langle \hat{c}_{\kappa s K}^\dagger \hat{c}_{\mu s J} \rangle^{\text{corr}} \\ &- \langle \hat{n}_{\mu \bar{s} J} \rangle \langle \hat{c}_{\mu s I}^\dagger \hat{c}_{\kappa s K} \rangle^{\text{corr}}] + Q_{\mu\nu, s}^{IJ}. \end{aligned} \quad (7)$$

The first two lines of Eq. (7) delineate the correlators' unhindered evolution and their interplay with site-local quantities. The last two lines introduce terms designed to preserve the trace-free nature of the correlators, consequently fostering coupling among the modes, as detailed below. Formally, this amounts to a minor correction of order $O(1/Z^2)$ and can be safely disregarded to leading order. The interactions with three-site correlations are encapsulated in $Q_{\mu\nu, s}^{IJ}$, also manifesting at the order of $O(1/Z^2)$. We have omitted considerations of particle-number correlations and spin correlators. Their dynamics unfold at a slower pace compared to the dynamics of doublon and holon excitations, hence assuming a subordinate role in the equilibration process.

B. Normal state

We consider the Hubbard system (1) to be at half filling in the strong-coupling limit with a large U . In this limit, a small, finite temperature would not generate doublon-holon pairs but would tend to disrupt the spin order within the system. This motivates the following ansatz for the site-local density matrix:

$$\begin{aligned} \hat{\rho}_\mu &= \left(\frac{1}{2} - \mathfrak{D}\right) (|\uparrow\rangle_\mu \langle \uparrow| + |\downarrow\rangle_\mu \langle \downarrow|) \\ &+ \mathfrak{D} (|\uparrow\downarrow\rangle_\mu \langle \uparrow\downarrow| + |0\rangle_\mu \langle 0|). \end{aligned} \quad (8)$$

Here, \mathfrak{D} represents the double occupancy in the Hubbard system, which is zero before the quench dynamics. If T takes a finite value, correlations among lattice sites are generated, resulting in a nonzero double occupancy. The dynamics can be determined from the local evolution equation (6), which, in Fourier space, reads

$$i\partial_t \mathfrak{D} = \sum_s \int_{\mathbf{k}} T_{\mathbf{k}} [f_s^{01}(T_{\mathbf{k}}) - f_s^{10}(T_{\mathbf{k}})]. \quad (9)$$

Here, $f_{\mathbf{k}, s}^{IJ}$ denote the Fourier components of the two-site correlators $\langle \hat{c}_{\mu s I}^\dagger \hat{c}_{\nu s J} \rangle^{\text{corr}}$, where we have assumed spatial homogeneity. Similarly, for the spatially homogeneous quench scenario under consideration, the \mathbf{k} dependence solely stems from the Fourier transformation $T_{\mathbf{k}}$ of the hopping matrix $T_{\mu\nu}$, which simplifies the momentum dependence $f_{\mathbf{k}, s}^{IJ} = f_s^{IJ}(T_{\mathbf{k}})$ of the correlation functions (up to the accuracy we are interested in).

This permits the usage of the spectral function $\sigma_d(\omega)$. For a hypercubic lattice in d dimensions, we find

$$\begin{aligned} \sigma_d(\omega) &= \int_{\mathbf{k}} \delta(\omega - T_{\mathbf{k}}) \\ &= \frac{1}{2\pi} \int_{-\infty}^{\infty} dx e^{ix\omega} \left[\mathcal{J}_0\left(\frac{T_x}{d}\right) \right]^d, \end{aligned} \quad (10)$$

where \mathcal{J}_0 denotes a Bessel function of the first kind. Then, relation (9) takes the form

$$i\partial_t \mathfrak{D} = \sum_s \int_{-T}^T d\omega \sigma_d(\omega) \omega [f_s^{01}(\omega) - f_s^{10}(\omega)]. \quad (11)$$

This simplifies the evaluation of a d -dimensional momentum integral in (9) to the evaluation of a one-dimensional integral in (11). Note that this simplification can be used

only when neglecting spin correlations. Similarly, the equations of motion for the two-site correlators can be written as

$$\begin{aligned}
 & (i\partial_t + [I - J]U)f_s^{IJ}(\omega) \\
 &= \frac{\omega}{2} \sum_L [f_s^{LJ}(\omega) - f_s^{IL}(\omega)] \\
 & - \frac{1}{2} \int_{-T}^T d\omega' \sigma_d(\omega') \omega' \sum_L [f_s^{LJ}(\omega') - f_s^{IL}(\omega')] \\
 & + \omega(\delta^{J1} - \delta^{I1}) \left(\mathfrak{D} - \frac{1}{4} \right) + Q_s^{IJ}(\omega). \quad (12)
 \end{aligned}$$

The first line of (12) determines the free evolution of the individual modes. The trace-free condition of the correlators leads to the coupling of the modes, which is taken care of in the second line. The primary source term of the correlators at leading order in the third line arises from the lattice filling, with a minor correction introduced by the double occupancy. Contributions from the interactions of three-point correlators are encapsulated in $Q_s^{IJ}(\omega)$.

III. QUENCH DYNAMICS

In the upcoming discussion, we examine a quantum quench within the Mott regime, transitioning from $T = 0$ to $T/U \ll 1$. Given that the hierarchy of the equations of motion is effectively managed by a small expansion parameter $1/Z$, we can systematically include higher-order terms in our analysis. Subsequently, we will delve into the analysis of prethermalization dynamics, employing various levels of approximation within this hierarchical expansion.

A. Free quasiparticle evolution

Considering the first order in $1/Z$, we can disregard the coupling to the double occupancy and also omit the coupling among the modes in Eq. (12), as they are formally of order $1/Z^2$, as shown in relation (7). We can significantly simplify the analysis by transforming the correlators into a diagonal basis that corresponds to the doublon and holon excitations. We achieve this by employing the Bogoliubov transformation $f_{s\omega}^{ab} = \sum_{IJ} O_\omega^{aI} O_\omega^{bJ} f_{s\omega}^{IJ}$, where the matrix is defined as

$$O_\omega^{aI} = \begin{pmatrix} \cos \varphi_\omega & \sin \varphi_\omega \\ -\sin \varphi_\omega & \cos \varphi_\omega \end{pmatrix}, \quad (13)$$

along with the rotation angle, given by

$$\tan \varphi_\omega = \frac{\sqrt{\omega^2 + U^2} + U}{\omega}. \quad (14)$$

In the rotated frame, the free evolution of the correlators (12) is described as follows:

$$i\partial_t f_s^{ab}(\omega) = [E_\omega^b - E_\omega^a] (f_s^{ab}(\omega) - \frac{1}{2} O_\omega^{a1} O_\omega^{b1}). \quad (15)$$

Here, we introduce the quasiparticle energies of doublons and holons, given by [54,60–65]

$$E_\omega^\pm = \frac{1}{2}(U - \omega \pm \sqrt{\omega^2 + U^2}). \quad (16)$$

The rapidly varying correlators f_s^{+-} and f_s^{-+} experience a rate of change of order U , while the quantities f_s^{--} and f_s^{++} do not display temporal evolution within the leading-order approach. We identify f_s^{--} and f_s^{++} as the distribution functions of doublon and holon excitations in the Mott-Hubbard system. The distribution functions exhibit nontrivial dynamics when accounting for the back-reaction of the correlators onto the mean field, as discussed in the next section. Certainly, it is worth noting that the long-term dynamics, specifically the relaxation of these distribution functions towards a thermal equilibrium state, can be comprehended within the hierarchical expansion at order $O(1/Z^3)$. Within this framework, a set of Boltzmann equations for the distribution functions can be derived, as demonstrated in [52,53]. However, since the Boltzmann evolution occurs considerably after the prethermalization dynamics, we will not delve into the associated scattering processes here.

The rapidly fluctuating doublon-holon correlations, denoted as $f_s^{+-} = [f_s^{-+}]^*$, govern the temporal evolution of correlations among lattice sites. This determines the equilibration of correlators among different lattice sites. Following some algebraic manipulation, we determine that, at leading order, the temporal evolution of the two-site correlators can be expressed in closed form, namely,

$$\begin{aligned}
 \langle \hat{\delta}_{\mu s}^\dagger \hat{\delta}_{\nu s} \rangle^{\text{corr}} &= \int_{\mathbf{k}} \frac{T_{\mathbf{k}} U}{2(T_{\mathbf{k}}^2 + U^2)} \\
 &\times (1 - \cos[\sqrt{U^2 + T_{\mathbf{k}}^2} t]) e^{i\mathbf{k} \cdot (\mathbf{x}_\mu - \mathbf{x}_\nu)}. \quad (17)
 \end{aligned}$$

Hence, the dephasing of the individual modes leads to the equilibration of site correlations, converging to a stationary value on the order of $O(T/U)$. Since the correlators influence the mean-field background through relation (9), the probability of having a nonvanishing double occupancy becomes nonzero,

$$\begin{aligned}
 \mathfrak{D}(t) &= \int_{\mathbf{k}} \frac{T_{\mathbf{k}}^2}{T_{\mathbf{k}}^2 + U^2} (1 - \cos[\sqrt{U^2 + T_{\mathbf{k}}^2} t]) \\
 &= \int_{-T}^T d\omega \frac{\sigma_d(\omega) \omega^2}{U^2 + \omega^2} (1 - \cos[\sqrt{U^2 + \omega^2} t]). \quad (18)
 \end{aligned}$$

We computed the oscillatory dynamics for two, three, and five dimensions, as shown in Fig. 1. To estimate the asymptotic decay of the oscillations to the quasistationary value of order $O(T^2/U^2)$, we perform an asymptotic expansion of the integral (18). By employing the spectral density given in (10), we deduce a power-law decay as follows:

$$\lim_{t \rightarrow \infty} \mathfrak{D}(t) - \mathfrak{D}_{\text{asym}} \approx \frac{T^2}{U^2} \left(\frac{\tau}{t} \right)^{d/2} f(t), \quad (19)$$

where $f(t)$ is a highly oscillating function with a magnitude of order unity and $\tau = O(U/T^2)$ denotes the timescale on which the oscillations decline.

Note that the above scaling (19) follows from the linearized quasiparticle evolution, which is the leading order in $1/Z$. Next-to-leading-order effects will be discussed in the next sections.

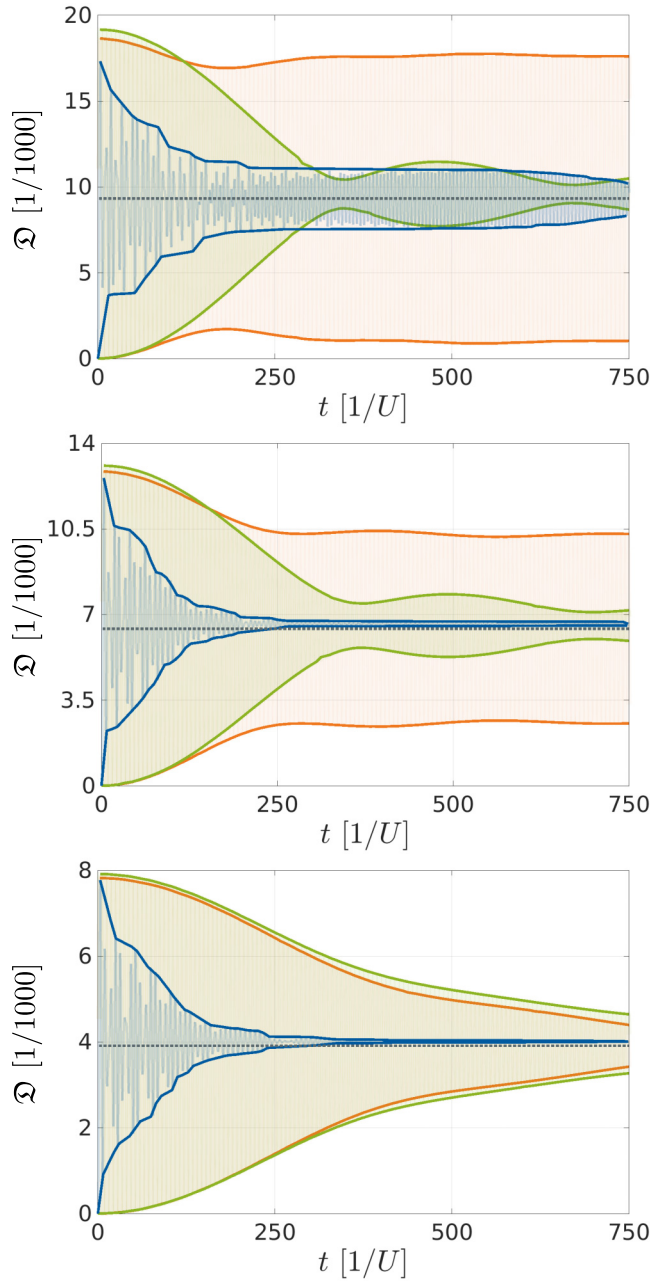


FIG. 1. Prethermalization dynamics of the double occupancy \mathcal{D} following a quench from $T = 0$ to $T/U = 0.2$ in two (top), three (middle), and five (bottom) dimensions. The dynamics exhibit rapid oscillations; therefore, we depict the envelope function illustrating the decay of the magnitude of the oscillations. The green curve represents the decay when only the free quasiparticle evolution is considered, as per Eq. (18). Adding the back-reaction of the correlations to the local mean field gives rise to the orange envelope. When considering three-point correlations in the dynamics, the blue envelope represents the decay of the correlators. The gray dotted line represents the asymptotic value $\mathcal{D}_{\text{asym}}$, as described in Eq. (24).

B. Back-reaction

The first departure from the free quasiparticle evolution involves the coupling to the double occupancy and inter-mode coupling. By applying the Bogoliubov transformation

from Eq. (12) and using the particle-hole symmetry $f_s^{00}(\omega) = -f_s^{11}(-\omega)$, we derive the dynamics for the correlators

$$i\partial_t f_s^{\text{ab}}(\omega) = [E_\omega^{\text{b}} - E_\omega^{\text{a}}] \left(f_s^{\text{ab}}(\omega) + 2O_\omega^{\text{a1}} O_\omega^{\text{b1}} \left[\mathcal{D} - \frac{1}{4} \right] \right) + \frac{i}{4} \sum_I (-1)^I O_\omega^{\text{aI}} O_\omega^{\text{bI}} \partial_t \mathcal{D}. \quad (20)$$

Each mode couples to the double occupancy. As the time dependence of these forced oscillations is the same for each mode, there is a partial restoration of the coherences, altering the prethermalization process. To quantify the correction to the leading-order analysis, we solve the system (20) along with (11) by utilizing Laplace transformations. This yields $\mathcal{D}(t) = \mathcal{L}^{-1}(\tilde{\mathcal{D}}(r))$, where the Laplace transform of the double occupancy is given by

$$\tilde{\mathcal{D}}(r) = \frac{1}{r} \frac{\mathcal{J}(r)}{1 + 3\mathcal{J}(r)}, \quad (21)$$

along with the integral

$$\mathcal{J}(r) = \int_{-T}^T d\omega \sigma_d(\omega) \frac{\omega^2}{r^2 + \omega^2 + U^2}. \quad (22)$$

In the regime of strong interactions, the correction to the averaged value for the double occupancy (18) is relatively small, approximately on the order of $O(T^4/U^4)$. However, there are notable alterations in the dynamics, particularly in two and three dimensions, while the corrections in higher dimensions (greater than three) are comparatively minor.

To be more specific, let us first discuss the case of two dimensions (top panel of Fig. 1). Just considering the free quasiparticle evolution (green curves), we see some beating effects but a clear signature of prethermalization (as expected). However, taking into account the back-reaction of these quasiparticle fluctuations onto the mean field (i.e., the double occupancy), we do not observe prethermalization anymore (orange curves), merely a slight initial decline in the magnitude of oscillations. As an intuitive picture, the coupling of the double occupancy to each mode restores coherences of local quantities, which weakens the effect of dephasing.

This effect of coherence restoration is also evident in three dimensions (middle panel of Fig. 1), albeit with a somewhat stronger initial decay in magnitude. Consequently, we conclude that especially in lower dimensions, it is crucial to consider higher-order correlators to accurately describe the prethermalization dynamics (blue curves in Fig. 1; see the next section).

In dimensions larger than three, the correction resulting from the back-reaction is significantly less pronounced. Surprisingly, it even amplifies the decay of oscillations compared to free evolution, as depicted in the lower panel of Fig. 1.

We conclude that the accuracy of the hierarchical expansion for temporal evolution is highly contingent on spatial dimension and the chosen order of approximation. Although in low dimensions higher-order correlators are essential for accurately describing the temporal evolution of local quantities, the asymptotic value can still be approximated if only two-site correlators and site-local dynamics are taken into account.

This observation holds true for the distribution functions representing doublon and holon excitations as well. Considering that we commence the time evolution in the Mott insulating state at $T = 0$, the initial conditions dictate $f_s^- = f_s^+ = 0$. Upon quenching the system to a finite value of T/U , these quasiparticle distributions also attain finite values. In fact, their prethermal values exhibit the same magnitude as the local double occupancy, namely,

$$f_{s,\text{asym}}^-(\omega) = \frac{U \mathcal{D}_{\text{asym}}}{4\sqrt{\omega^2 + U^2}} = -f_{s,\text{asym}}^+(\omega). \quad (23)$$

These expressions, which are formally asymptotic, serve as the foundation for the distribution functions of doublons and holons, initiating the slow long-term dynamics. During the prethermalization process, it is difficult to assert that f_s^- and f_s^+ represent well-defined quasiparticle distributions, given their highly oscillatory nature. Only as the temporal evolution approaches the prethermal state do these distribution functions accurately describe slow variables. Therefore, the prethermalization process is essential to achieve the separation of timescales. Initially, there is rapid oscillatory behavior, followed by a subsequent slow evolution, where a Boltzmann description becomes applicable. In essence, by using the hierarchical equations of motion we do not assume the existence of quasiparticles beforehand. Instead, the temporal evolution reveals the relevant slow-evolving variables directly [52,53,66]. However, it is evident that for two and three spatial dimensions, a viable description of the equilibration process necessitates considering higher-order correlations. As discussed below, even in this scenario, the average value of \mathcal{D} aligns with its asymptotic value. Formally, the asymptotic value for the double occupancy can be straightforwardly deduced from the Laplace transform (21), yielding

$$\mathcal{D}_{\text{asym}} = \frac{\Im(0)}{1 + 3\Im(0)}. \quad (24)$$

Note that this expression is formally bounded by the infinite-temperature value, i.e., $\mathcal{D}_{\text{asym}} < 1/4$. Comparing this with the leading-order result of $\mathcal{D}_{\text{asym}}$ obtained from (18), we observe that the correction due to the back-reaction is of order $O(T^4/U^4)$. As one might expect, the two-site correlations also experience a small correction,

$$\langle \hat{c}_{\mu s}^\dagger \hat{c}_{\nu s} \rangle_{\text{asym}}^{\text{corr}} = \int_{\mathbf{k}} \frac{UT_{\mathbf{k}}}{2(T_{\mathbf{k}}^2 + U^2)} \frac{e^{i\mathbf{k} \cdot (\mathbf{x}_\mu - \mathbf{x}_\nu)}}{1 + 3\Im(0)}. \quad (25)$$

We want to stress that even though we took the formal limit of $t \rightarrow \infty$ to derive the prethermal values, our analysis does not encompass the scenario of infinitely long times. As mentioned earlier, to investigate the long-time dynamics, it is necessary to consider scattering processes between quasiparticles. These processes can be addressed using Boltzmann equations that involve four-site correlators, which are of order $O(1/Z^3)$.

C. Three-point correlators

We emphasize the necessity of considering higher-order correlators to obtain a reasonable description of the prethermalization dynamics, especially in two and three dimensions. The dominant three-site correlators, which contribute to the source term $Q_{\mu\nu s}^J$ in Eq. (7), are given for pairwise distinct

sites as follows:

$$\langle \hat{n}_{\lambda\bar{s}K} \hat{c}_{\mu s I}^\dagger \hat{c}_{\nu s J} \rangle^{\text{corr}} = \langle \hat{n}_{\alpha\bar{s}K} \hat{c}_{\mu s I}^\dagger \hat{c}_{\nu s J} \rangle - \langle \hat{n}_{\alpha\bar{s}K} \rangle \langle \hat{c}_{\mu s I}^\dagger \hat{c}_{\nu s J} \rangle, \quad (26)$$

$$\langle \hat{c}_{\lambda,s}^\dagger \hat{c}_{\lambda,\bar{a}} \hat{c}_{\mu\bar{s}I}^\dagger \hat{c}_{\nu s J} \rangle^{\text{corr}} = \langle \hat{c}_{\lambda,a}^\dagger \hat{c}_{\lambda,\bar{a}} \hat{c}_{\mu\bar{s}I}^\dagger \hat{c}_{\nu s J} \rangle, \quad (27)$$

$$\langle \hat{c}_{\lambda,s}^\dagger \hat{c}_{\lambda,s} \hat{c}_{\mu\bar{s}I}^\dagger \hat{c}_{\nu s J} \rangle^{\text{corr}} = \langle \hat{c}_{\lambda,s}^\dagger \hat{c}_{\lambda,s} \hat{c}_{\mu\bar{s}I}^\dagger \hat{c}_{\nu s J} \rangle. \quad (28)$$

Note that these simple expressions rely on the symmetries of our setup, such as vanishing spin polarization, which implies $\langle \hat{c}_{\mu\bar{s}I}^\dagger \hat{c}_{\nu s J} \rangle = 0$.

These correlators are described by equations of motion that involve couplings to two-site correlations, double occupancy, and higher-order correlators (see Appendix A for details). The resulting equations of motion are highly nonlinear, disrupting coherences among individual modes and driving local quantities towards a long-lived prethermal state. In dimensions 2 and 3, the effect of coherence restoration due to the back-reaction is surpassed, leading to a significant decrease in the magnitude of the oscillations, as illustrated in Fig. 1.

The site-local dynamics are driven by hopping events of holon and doublon excitations. As the return probability to a particular site diminishes with higher dimensionality, coherent oscillations decay more rapidly in higher dimensions. This observation is consistent with our results, where after incorporating the three-point correlators, the equilibration process accelerates in dimensions 3 and 5 compared to the two-dimensional setting.

IV. BANDWIDTH SCALING

In Fig. 1 we compare the prethermalization dynamics in different dimensions, but for the same values of T and U in Eq. (1). However, such a comparison requires special care because the impact of the hopping term $\propto T$ in Eq. (1) strongly depends on the lattice structure, e.g., the dimensionality of the lattice, in contrast to the on-site repulsion U . Keeping T fixed as in Fig. 1 means that the total bandwidth remains constant. The extremal values of $\pm T$ are reached in the corners of the Brillouin zone. However, in the limit of large dimensions, the probability of being in those corners (i.e., their relative weight in the spectral density σ_d) becomes very small, and thus, it is useful to introduce an effective bandwidth. In view of the central limit theorem, the spectral density σ_d (i.e., the density of states) approaches a Gaussian distribution. Its standard deviation scales with T/\sqrt{Z} and can be identified with an effective bandwidth. Actually, this line of argument underlies the well-known method of dynamical mean-field theory (DMFT; see, e.g., [57,67]).

In order to disentangle the dependence on bandwidth and dimension better, we compare three different scaling laws in Fig. 2. The left column is exactly the same as in Fig. 1, where T , i.e., the total bandwidth, is kept constant. In the middle column, the effective bandwidth, i.e., T/\sqrt{Z} , is kept constant, which corresponds to the scaling used in DMFT. Finally, the right column corresponds to the case where T/Z , i.e., the prefactor in front of the hopping term in Eq. (1), is kept constant. In order to facilitate a comparison between the three columns (i.e., from left to right), we used the case of three dimensions as a reference; i.e., the middle row displays the same plot three times. As a result, T decreases from left

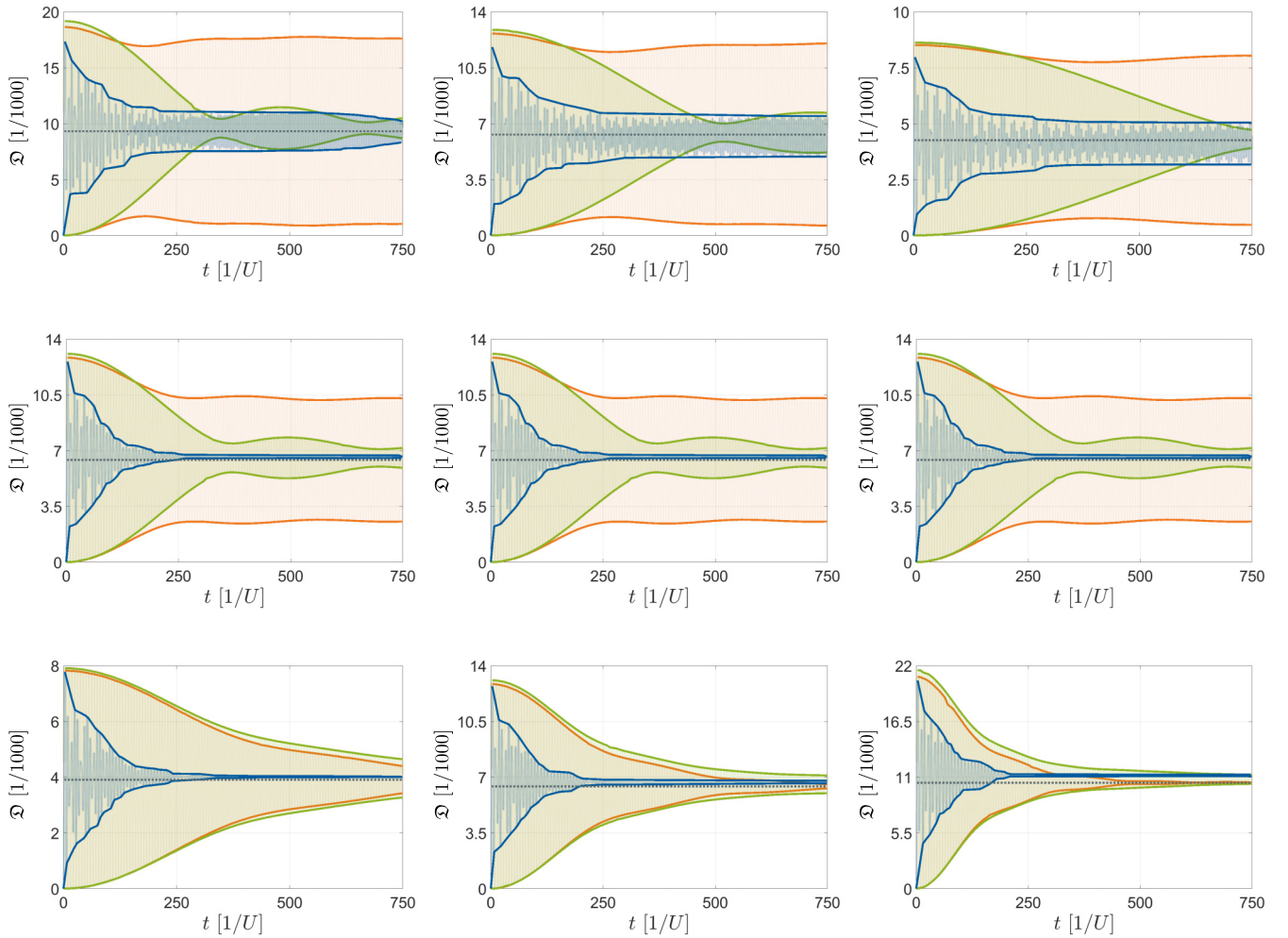


FIG. 2. Prethermalization dynamics of the double occupancy \mathcal{D} following a quench in two (top row), three (middle row), and five (bottom row) dimensions as in Fig. 1, but applying different scaling laws of the bandwidth with Z . The left column is exactly the same as in Fig. 1; i.e., the hopping strength T is kept fixed. In the middle column, T is adapted such that T/\sqrt{Z} remains constant, where its value in three dimensions (middle row) is kept fixed for comparison. In the right column, T is scaled such that T/Z remains constant. Thus, in the top row, T decreases from left to right, whereas in the bottom row, T increases from left to right (in the middle row, it stays constant; see Fig. 3 in Appendix B)

to right in the top row, while it is the other way around in the bottom row.

As expected, the prethermalization dynamics following from the linearized quasiparticle evolution (green curves) occurs faster for larger T . In five dimensions, the same tendency is observable when including back-reaction (orange curves). In two dimensions, on the other hand, including back-reaction (orange curves) yields a strong slowdown of prethermalization. Thus, the impact of back-reaction becomes weaker for higher dimensions. As another observation, the magnitude of the double occupancy in the steady state remains approximately constant in the middle column, which can be seen as a signature of the DMFT limit $Z \rightarrow \infty$. Furthermore, the characteristic timescale $tU \approx 250$ of prethermalization one can read off the blue curves (in the middle column) is nearly the same in three and five dimensions, which is another smoking gun of the DMFT limit $Z \rightarrow \infty$. It can be demonstrated using Eq. (18) that in this limit and keeping T/\sqrt{Z} constant, the oscillations of the double occupancy exhibit exponential decay, approximately characterized by $\sim \exp(-T^2 t^2/Z)$.

A. Comparison to dynamical mean-field theory

At this point it might be adequate to compare the two methods, i.e., the hierarchy of correlations used here and DMFT. As explained above, DMFT is usually based on a different scaling with coordination number Z , namely, $1/\sqrt{Z}$ instead of $1/Z$ as in Eq. (1). As a result, the limit $Z \rightarrow \infty$ is already non-trivial in DMFT. In our approach, this limit is much simpler since all the correlations vanish and the state basically boils down to a product of the local on-site density matrices (8) describing the mean-field background. This simplicity allows us to derive the $1/Z$ corrections which contain interesting physics such as prethermalization. Therefore, the hierarchy of correlations facilitates studying the impact of the structure and dimensionality of the lattice, which is much harder in DMFT.

As another point, since DMFT effectively maps the whole lattice onto a single-site problem, it is harder to retrieve important information regarding the spatial structures (e.g., the \mathbf{k} dependence). Finally, DMFT is a dominantly numerical approach, while the hierarchy of correlations

facilitates analytical approximations, showing that they are complementary methods.

V. CONCLUSIONS

Via the hierarchy of correlations, we investigated the prethermalization dynamics in the Mott insulator state of the strongly interacting Fermi-Hubbard model after a hopping quench. As a starting point, we focused on the free quasiparticle evolution as encoded in the two-point correlation functions, which yields the usual prethermalization picture.

We found that prethermalization can take a comparably long period of time $\Delta t \gg 1/U$, i.e., much longer than what is expected from other works; see, e.g., [10,68–71], where only a few oscillations were required until the prethermal state was approached. We attribute this difference to two main reasons: First, we consider a hopping quench where T is switched from zero to a small value (still well within the Mott insulator regime) instead of an interaction quench where U is switched. Switching U from zero (i.e., the metallic state) to a final value in the Mott insulator regime yields a strong excitation, i.e., a large number of quasiparticles, whereas the hopping quench considered here creates a much smaller number of quasiparticles. Second, the final state in our quench scenario is deep inside the Mott insulator regime characterized by a large Mott gap $\approx U$ and a small quasiparticle bandwidth $\propto T$. The Mott gap yields a base frequency for the oscillations, while their dephasing is generated by the small bandwidth $\propto T$. Actually, as becomes evident from Eq. (18), this dephasing is further slowed down by the fact that it is governed by the term in the square root of the dispersion relation which is quadratic in T . This is consistent with the observation that prethermalization in the Bose-Hubbard model can occur faster (see, e.g., [22,58]). The speedup can be partially attributed to the different dispersion relation of the Bose-Hubbard model, where the square root also contains a contribution linear in the hopping strength $T_{\mathbf{k}}$.

In view of this comparably long timescale $\Delta t \gg 1/U$, small corrections to this leading order might become important because they could accumulate over time. Taking into account the first nontrivial correction to this leading order, i.e., the back-reaction of the quasiparticle fluctuations onto the mean-field background, we found that this effect significantly suppresses prethermalization, especially in lower dimensions. As an intuitive picture, the joint coupling of all the quasiparticle modes to the same mean-field mode introduces additional coherences between them and reduces their dephasing.

We also included three-point correlations (i.e., further higher-order effects) in our approach. Their impact tends to enhance prethermalization (even stronger than the suppression due to back-reaction), which can be explained by the fact that they mediate nonlinear interactions between the quasiparticle modes, which in turn can result in a more efficient scrambling of their phases.

Note, however, that all these results are still within the realm of prethermalization; i.e., none of these effects can describe full thermalization. On the leading-order level of the linearized quasiparticle evolution, this becomes evident from the fact that the quasiparticle distribution functions do not change after the quench—only their oscillations become

out of phase. Thus, unless these distribution functions are accidentally thermal directly after the quench (which is not the case here and would require a very finely tuned stimulus), the steady state is not thermal. The same argument applies when taking into account back-reaction because the quasiparticle distribution functions change by only a global factor. Including the three-point correlations complicates the situation a bit, but the main conclusion remains correct: Even though local quantities such as the double occupancy of a lattice site approach a steady state, the expectation values of \mathbf{k} -dependent operators (which should be stationary in a thermal state) still oscillate. For finite lattices with discrete \mathbf{k} , these oscillations can manifest as revivals.

Full thermalization occurs on much longer timescales on which the quasiparticle distribution functions change via Boltzmann-type collisions. Describing them requires incorporating the four-point correlations (cf. [52–54]).

In summary, we found that, depending on the involved parameters, the relaxation dynamics of this strongly interacting quantum many-body system can occur in several stages in which different mechanisms play a role. As explained in the Introduction, prethermalization is a quite generic phenomenon, and thus, we expect that our results can, at least qualitatively, also be found in other systems undergoing fast switching processes. For example, other systems could also feature relaxation times which are much longer than expected at first glance, especially if not all parameters are of similar magnitude. The back-reaction of the quasiparticle fluctuations onto the background and the impact of higher-order correlations should also play a role in other systems, and one might even expect that their tendency to slow down or speed up prethermalization is similar to what is found here. However, this requires further studies which would then further complete our understanding of relaxation phenomena.

ACKNOWLEDGMENTS

This work was funded by the Deutsche Forschungsgemeinschaft (DFG, German Research Foundation), Project ID No. 278162697–SFB 1242.

APPENDIX A: THREE-POINT CORRELATORS

We consider only the particular case when the momentum dependence of the Fourier components of the correlators is solely determined by the hopping matrix $T_{\mathbf{k}}$. Then we can employ for the correlators (26)–(28) the expansions

$$\langle \hat{n}_{\lambda,s} \hat{c}_{\mu,I}^\dagger \hat{c}_{\nu,S} \rangle^{\text{corr}} = \int_{\mathbf{k},\mathbf{p}} g_{\bar{s}s}^{KIJ}(T_{\mathbf{k}}, T_{\mathbf{p}}) e^{i\mathbf{k} \cdot (\mathbf{x}_\mu - \mathbf{x}_\lambda) + i\mathbf{p} \cdot (\mathbf{x}_\nu - \mathbf{x}_\lambda)}, \quad (\text{A1})$$

$$\langle \hat{c}_{\lambda,s}^\dagger \hat{c}_{\lambda,\bar{s}} \hat{c}_{\mu,I}^\dagger \hat{c}_{\nu,S} \rangle^{\text{corr}} = \int_{\mathbf{k},\mathbf{p}} r_{\bar{s}s}^{IJ}(T_{\mathbf{k}}, T_{\mathbf{p}}) e^{i\mathbf{k} \cdot (\mathbf{x}_\mu - \mathbf{x}_\lambda) + i\mathbf{p} \cdot (\mathbf{x}_\nu - \mathbf{x}_\lambda)}, \quad (\text{A2})$$

$$\langle \hat{c}_{\lambda,s}^\dagger \hat{c}_{\lambda,\bar{s}}^\dagger \hat{c}_{\mu,I} \hat{c}_{\nu,S} \rangle^{\text{corr}} = \int_{\mathbf{k},\mathbf{p}} h_{\bar{s}s}^{IJ}(T_{\mathbf{k}}, T_{\mathbf{p}}) e^{i\mathbf{k} \cdot (\mathbf{x}_\mu - \mathbf{x}_\lambda) + i\mathbf{p} \cdot (\mathbf{x}_\nu - \mathbf{x}_\lambda)}. \quad (\text{A3})$$

Employing the spectral density, we obtain for the source term in (12) the expression

$$\begin{aligned}
 Q_s^{IJ}(\omega) &= \sum_K \int_{-T}^T d\omega' \sigma_d(\omega') \omega' [g_{\bar{s}s\bar{s}}^{KJ}(\omega', \omega) - g_{\bar{s}s\bar{s}}^{IK}(\omega, \omega')] \\
 &+ (-1)^I \sum_K \int_{-T}^T d\omega' \sigma_d(\omega') \omega' [r_{\bar{s}s}^{KJ}(\omega', \omega) + h_{\bar{s}s}^{KJ}(\omega', \omega)] \\
 &- (-1)^J \sum_K \int_{-T}^T d\omega' \sigma_d(\omega') \omega' \{ [r_{\bar{s}s}^{KI}(\omega', \omega)]^* \\
 &+ [h_{\bar{s}s}^{KI}(\omega, \omega')]^* \}. \tag{A4}
 \end{aligned}$$

For the first set of three-point correlators, the equation of motion reads

$$\begin{aligned}
 (i\partial_t + [I - J]U) g^{KIJ}(\omega_1, \omega_2) &= \frac{\omega_1}{2} \sum_L g_{\bar{s}s\bar{s}}^{KLJ}(\omega_1, \omega_2) - \frac{\omega_2}{2} \sum_L g_{\bar{s}s\bar{s}}^{KIL}(\omega_1, \omega_2) \\
 &+ \frac{(-1)^K}{4} \omega_1 [f_s^{0J}(\omega_2) - f_s^{1J}(\omega_2)] \\
 &- \frac{(-1)^K}{4} \omega_2 [f_s^{0I}(\omega_1) - f_s^{1I}(\omega_1)] \\
 &- \frac{1}{2} \int_{-T}^T d\omega \sigma_d(\omega) \omega \sum_L [g_{\bar{s}s\bar{s}}^{KLJ}(\omega, \omega_2) \\
 &- g_{\bar{s}s\bar{s}}^{KIL}(\omega_1, \omega)]. \tag{A5}
 \end{aligned}$$

The last line ensures the sum rules $\int d\omega \sigma_d(\omega) g_{\bar{s}s\bar{s}}^{KIJ}(\omega, \omega_2) = \int d\omega \sigma_d(\omega) g_{\bar{s}s\bar{s}}^{KIJ}(\omega_1, \omega) = 0$ which follow from the requirement that the three-point correlators have to vanish if two sites coincide. The equation of motion for the second set of three-point correlators contains bilinear couplings among the two-site correlators. It reads explicitly

$$\begin{aligned}
 (i\partial_t + [I - J]U) r_{\bar{s}s}^{IJ}(\omega_1, \omega_2) &= \frac{\omega_1}{2} \sum_L r_{\bar{s}s}^{LJ}(\omega_1, \omega_2) - \frac{\omega_2}{2} \sum_L r_{\bar{s}s}^{IL}(\omega_1, \omega_2) \\
 &+ \sum_{K,L} (\omega_1 - \omega_2) f_s^{KJ}(\omega_2) f_s^{IL}(\omega_1) \\
 &- \sum_L \left[(-1)^I \left(\mathfrak{D} - \frac{1}{4} \right) - \frac{1}{4} (-1)^L \right] \omega_1 f_s^{LJ}(\omega_2) \\
 &+ \sum_L \left[(-1)^J \left(\mathfrak{D} - \frac{1}{4} \right) - \frac{1}{4} (-1)^L \right] \omega_2 f_s^{IL}(\omega_1) \\
 &- \frac{1}{2} \int_{-T}^T d\omega \sigma_d(\omega) \omega \sum_L [r_{\bar{s}s}^{LJ}(\omega, \omega_2) - r_{\bar{s}s}^{IL}(\omega_1, \omega)] \\
 &- \int_{-T}^T d\omega \sigma_d(\omega) \omega \sum_{K,L} [f_s^{KJ}(\omega_2) f_s^{IL}(\omega) \\
 &- f_s^{KJ}(\omega) f_s^{IL}(\omega_1)]. \tag{A6}
 \end{aligned}$$

Again, the last two lines ensure the sum rules $\int d\omega \sigma_d(\omega) r_{\bar{s}s}^{IJ}(\omega, \omega_2) = \int d\omega \sigma_d(\omega) r_{\bar{s}s}^{IJ}(\omega_1, \omega) = 0$. Finally,

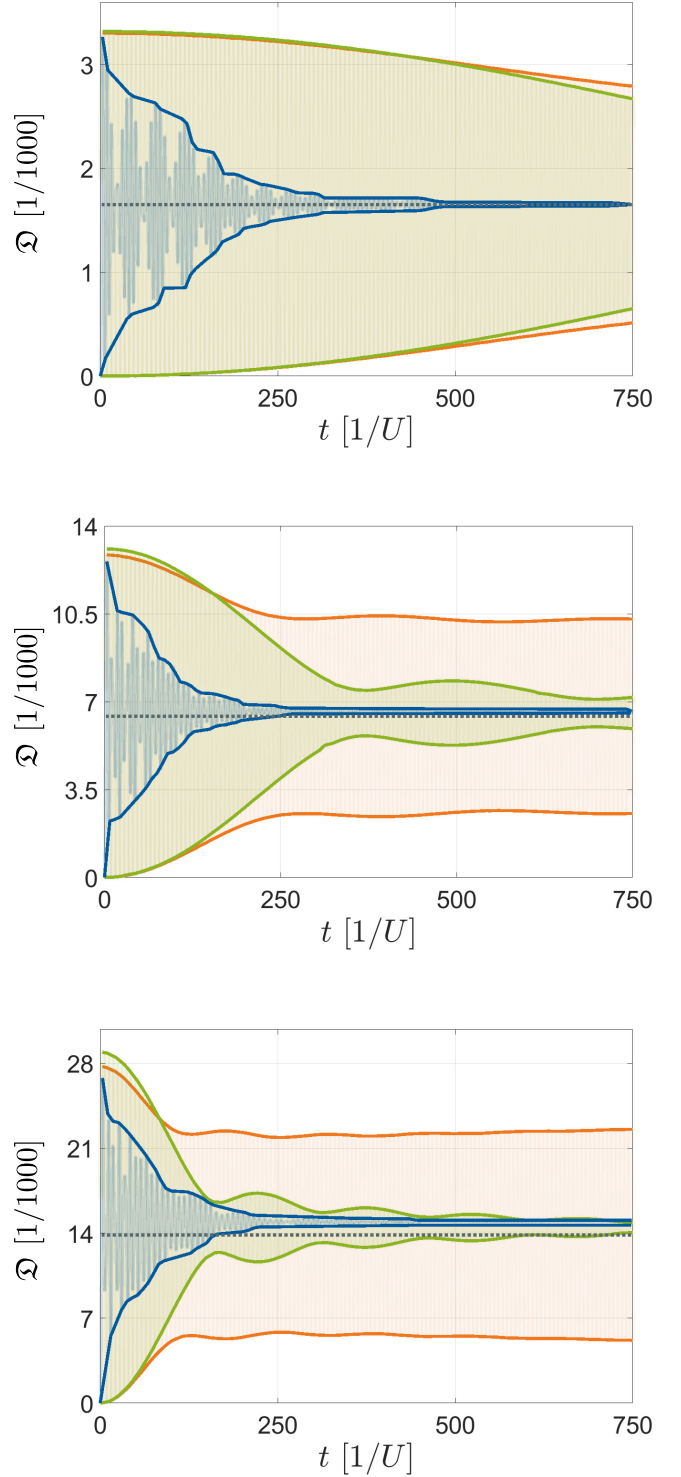


FIG. 3. Prethermalization dynamics of the double occupancy \mathfrak{Q} following a quench in three dimensions as in Figs. 1 and 2, but now for different values of T , with $T/U = 0.1$ (top), $T/U = 0.2$ (middle), and $T/U = 0.3$ (bottom).

we have for the third set of equations

$$\begin{aligned}
 (i\partial_t + [1 - I - J]U) h^{IJ}(\omega_1, \omega_2) &= -\frac{\omega_1}{2} \sum_L h^{LJ}(\omega_1, \omega_2) - \frac{\omega_2}{2} \sum_L h^{IL}(\omega_1, \omega_2)
 \end{aligned}$$

$$\begin{aligned}
& + \sum_{K,L} (\omega_1 + \omega_2) f_s^{KI}(\omega_1) f_s^{LJ}(\omega_2) \\
& + \omega_1 \sum_L \left[\frac{(-1)^L}{4} + (-1)^J \left(\frac{1}{4} - \mathfrak{D} \right) \right] f_s^{LJ}(\omega_2) \\
& + \omega_2 \sum_L \left[\frac{(-1)^L}{4} + (-1)^J \left(\frac{1}{4} - \mathfrak{D} \right) \right] f_s^{LJ}(\omega_1) \\
& + \frac{1}{2} \int_{-T}^T d\omega \sigma_d(\omega) \omega \sum_L \left[h_{ss}^{LJ}(\omega, \omega_2) + h_{ss}^{LL}(\omega_1, \omega) \right] \\
& - \int_{-T}^T d\omega \sigma_d(\omega) \omega \sum_{K,L} \left[f_s^{KI}(\omega_1) f_s^{LJ}(\omega) \right. \\
& \left. + f_s^{KI}(\omega) f_s^{LJ}(\omega_2) \right]. \tag{A7}
\end{aligned}$$

Also, here, the last two lines ensure the sum rules $\int d\omega \sigma_d(\omega) h_{ss}^{LJ}(\omega, \omega_2) = \int d\omega \sigma_d(\omega) h_{ss}^{LJ}(\omega_1, \omega) = 0$.

APPENDIX B: BANDWIDTH SCALING IN THREE DIMENSIONS

By direct comparison, the plots in Fig. 2 allow us to study the impact of Z and the scaling with Z , as well as the dependence on T in two and five dimensions, but they do not display the T dependence in three dimensions since T is kept constant in the middle row. In order to amend this drawback, we plot the T dependence in three dimensions in Fig. 3. As in Fig. 2, the prethermalization dynamics accelerates for growing T , i.e., from top to bottom (as expected).

As another point, we may compare the prethermalization dynamics in Fig. 3 with the timescales required for full thermalization, which can be obtained from the Boltzmann equation [50–54]. The precise Boltzmann thermalization dynamics depends on various details such as the (initial) quasiparticle distribution functions, but we may obtain an estimate via the well-known relaxation time approximation

(obtained by linearizing the Boltzmann equation) in the high-temperature limit (where one expects a fast relaxation). From the Boltzmann equation derived in [52,54] and using the fact that the spectral density approximately behaves as a Gaussian (see above), this procedure yields the relaxation time

$$\tau \sim \frac{U^2 Z^{3/2}}{T^3}. \tag{B1}$$

For the values of $T/U = 0.2$ (middle panel in Fig. 3) and $Z = 6$ (cubic lattice in three dimensions), we find a rather large relaxation timescale of $U\tau \sim 1800$, which is outside the range plotted in Fig. 3. This corroborates our earlier statement that full relaxation takes a longer time.

The scaling of τ in Eq. (B1) can be understood in the following way. After a hopping quench considered here, the density of created quasiparticles (i.e., doublons and holons) scales with T^2/U^2 . Since Boltzmann relaxation dynamics occurs via collisions between these quasiparticles, the corresponding rate is suppressed by this small density. Another factor of T stems from the collisional cross section in the Boltzmann equation [52,54], which explains the scaling of τ with U^2/T^3 . In order to understand the Z dependence in Eq. (B1), we may consider the DMFT scaling where T/Z in Eq. (1) is replaced by T/\sqrt{Z} . Using this scaling and considering the DMFT limit $Z \rightarrow \infty$, the resulting behavior (such as τ) does not depend on Z . Then, translating back to our scaling with T/Z in Eq. (1), we recover Eq. (B1).

Note that the ability to disentangle the various timescales for prethermalization in Fig. 3 from those of full thermalization τ is a feature of the scenario considered here (hopping quench within Mott phase). For other cases (e.g., interaction quenches), this separation of timescales may be less developed, and thus, it may be much harder to disentangle the various phenomena.

-
- [1] J. M. Deutsch, Quantum statistical mechanics in a closed system, *Phys. Rev. A* **43**, 2046 (1991).
 - [2] J. Berges, S. Borsányi, and C. Wetterich, Prethermalization, *Phys. Rev. Lett.* **93**, 142002 (2004).
 - [3] M. Srednicki, Chaos and quantum thermalization, *Phys. Rev. E* **50**, 888 (1994).
 - [4] J. Berges, S. Borsányi, and J. Serreau, Thermalization of fermionic quantum fields, *Nucl. Phys. B* **660**, 51 (2003).
 - [5] P. Calabrese and J. Cardy, Time dependence of correlation functions following a quantum quench, *Phys. Rev. Lett.* **96**, 136801 (2006).
 - [6] P. Calabrese, and J. Cardy, Quantum quenches in extended systems, *J. Stat. Mech.* (2007) P06008.
 - [7] M. Rigol, V. Dunjko, V. Yurovsky, and M. Olshanii, Relaxation in a completely integrable many-body quantum system: An *ab initio* study of the dynamics of the highly excited states of 1D lattice hard-core bosons, *Phys. Rev. Lett.* **98**, 050405 (2007).
 - [8] S. R. Manmana, S. Wessel, R. M. Noack, and A. Muramatsu, Strongly correlated fermions after a quantum quench, *Phys. Rev. Lett.* **98**, 210405 (2007).
 - [9] M. Rigol, V. Dunjko, and M. Olshanii, Thermalization and its mechanism for generic isolated quantum systems, *Nature (London)* **452**, 854 (2008).
 - [10] M. Eckstein, A. Hackl, S. Kehrein, M. Kollar, M. Moeckel, P. Werner, and F. A. Wolf, New theoretical approaches for correlated systems in nonequilibrium, *Eur. Phys. J. Spec. Top.* **180**, 217 (2009).
 - [11] M. Moeckel, and S. Kehrein, Real-time evolution for weak interaction quenches in quantum systems, *Ann. Phys. (NY)* **324**, 2146 (2009).
 - [12] M. A. Cazalilla, and M. Rigol, Focus on dynamics and thermalization in isolated quantum many-body systems, *New J. Phys.* **12**, 055006 (2010).
 - [13] A. Polkovnikov, K. Sengupta, A. Silva, and M. Vengalattore, Colloquium: Nonequilibrium dynamics of closed interacting quantum systems, *Rev. Mod. Phys.* **83**, 863 (2011).
 - [14] M. Kollar, F. A. Wolf, and M. Eckstein, Generalized Gibbs ensemble prediction of prethermalization plateaus and their relation to nonthermal steady states in integrable systems, *Phys. Rev. B* **84**, 054304 (2011).

- [15] T. Kitagawa, A. Imambekov, J. Schmiedmayer, and E. Demler, The dynamics and prethermalization of one-dimensional quantum systems probed through the full distributions of quantum noise, *New J. Phys.* **13**, 073018 (2011).
- [16] C. Gogolin, M. P. Müller, and J. Eisert, Absence of thermalization in nonintegrable systems, *Phys. Rev. Lett.* **106**, 040401 (2011).
- [17] M. C. Bañuls, J. I. Cirac, and M. B. Hastings, Strong and weak thermalization of infinite nonintegrable quantum systems, *Phys. Rev. Lett.* **106**, 050405 (2011).
- [18] M. Rigol and M. Srednicki, Alternatives to eigenstate thermalization, *Phys. Rev. Lett.* **108**, 110601 (2012).
- [19] M. Gring, M. Kuhnert, T. Langen, T. Kitagawa, B. Rauer, M. Schreitil, I. Mazets, D. A. Smith, E. Demler, and J. Schmiedmayer, Relaxation and prethermalization in an isolated quantum system, *Science* **337**, 1318 (2012).
- [20] J. Sirker, N. P. Konstantinidis, F. Andraschko, and N. Sedlmayr, Locality and thermalization in closed quantum systems, *Phys. Rev. A* **89**, 042104 (2014).
- [21] R. Steinigeweg, A. Khodja, H. Niemeyer, C. Gogolin, and J. Gemmer, Pushing the limits of the eigenstate thermalization hypothesis towards mesoscopic quantum systems, *Phys. Rev. Lett.* **112**, 130403 (2014).
- [22] S. Sorg, L. Vidmar, L. Pollet, and F. Heidrich-Meisner, Relaxation and thermalization in the one-dimensional Bose-Hubbard model: A case study for the interaction quantum quench from the atomic limit, *Phys. Rev. A* **90**, 033606 (2014).
- [23] P. Smacchia, M. Knap, E. Demler, and A. Silva, Exploring dynamical phase transitions and prethermalization with quantum noise of excitations, *Phys. Rev. B* **91**, 205136 (2015).
- [24] M. Babadi, E. Demler, and M. Knap, Far-from-equilibrium field theory of many-body quantum spin systems: Prethermalization and relaxation of spin spiral states in three dimensions, *Phys. Rev. X* **5**, 041005 (2015).
- [25] P. Calabrese and J. Cardy, Quantum quenches in 1 + 1 dimensional conformal field theories, *J. Stat. Mech.* (2016) 064003.
- [26] A. M. Kaufman, M. E. Tai, A. Lukin, M. Rispoli, R. Schittko, P. M. Preiss, and M. Greiner, Quantum thermalization through entanglement in an isolated many-body system, *Science* **353**, 794 (2016).
- [27] T. Langen, T. Gasenzer, and J. Schmiedmayer, Prethermalization and universal dynamics in near-integrable quantum systems, *J. Stat. Mech.* (2016) 064009.
- [28] C. Neill *et al.*, Ergodic dynamics and thermalization in an isolated quantum system, *Nat. Phys.* **12**, 1037 (2016).
- [29] T. Farrelly, F. G. S. L. Brandão, and M. Cramer, Thermalization and return to equilibrium on finite quantum lattice systems, *Phys. Rev. Lett.* **118**, 140601 (2017).
- [30] N. Schlünzen, J.-P. Joost, F. Heidrich-Meisner, and M. Bonitz, Nonequilibrium dynamics in the one-dimensional Fermi-Hubbard model: Comparison of the nonequilibrium Green-functions approach and the density matrix renormalization group method, *Phys. Rev. B* **95**, 165139 (2017).
- [31] B. Neyenhuis, J. Zhang, P. W. Hess, J. Smith, A. C. Lee, P. Richerme, Z.-X. Gong, A. V. Gorshkov, and C. Monroe, Observation of prethermalization in long-range interacting spin chains, *Sci. Adv.* **3**, e1700672 (2017).
- [32] P. W. Hess, P. Becker, H. B. Kaplan, A. Kyprianidis, A. C. Lee, B. Neyenhuis, G. Pagano, P. Richerme, C. Senko, J. Smith, W. L. Tan, J. Zhang, and C. Monroe, Non-thermalization in trapped atomic ion spin chains, *Philos. Trans. R. Soc. A* **375**, 20170107 (2017).
- [33] J. Marino, M. Eckstein, M. S. Foster, and A. M. Rey, Dynamical phase transitions in the collisionless pre-thermal states of isolated quantum systems: Theory and experiments, *Rep. Prog. Phys.* **85**, 116001 (2022).
- [34] A. Herrmann, Y. Murakami, M. Eckstein and P. Werner, Floquet prethermalization in the resonantly driven Hubbard model, *Europhys. Lett.* **120**, 57001 (2017).
- [35] S. A. Weidinger and M. Knap, Floquet prethermalization and regimes of heating in a periodically driven, interacting quantum system, *Sci. Rep.* **7**, 45382 (2017).
- [36] W. W. Ho, I. Protopopov, and D. A. Abanin, Bounds on energy absorption and prethermalization in quantum systems with long-range interactions, *Phys. Rev. Lett.* **120**, 200601 (2018).
- [37] M. R. C. Fitzpatrick and M. P. Kennett, Light-cone-like spreading of single-particle correlations in the Bose-Hubbard model after a quantum quench in the strong-coupling regime, *Phys. Rev. A* **98**, 053618 (2018).
- [38] I. Frérot, P. Naldesi, and T. Roscilde, Multispeed prethermalization in quantum spin models with power-law decaying interactions, *Phys. Rev. Lett.* **120**, 050401 (2018).
- [39] F. Peronaci, M. Schiró, and O. Parcollet, Resonant thermalization of periodically driven strongly correlated electrons, *Phys. Rev. Lett.* **120**, 197601 (2018).
- [40] F. Lange, Z. Lenarčič, and A. Rosch, Time-dependent generalized Gibbs ensembles in open quantum systems, *Phys. Rev. B* **97**, 165138 (2018).
- [41] K. X. Wei, P. Peng, O. Shtanko, I. Marvian, S. Lloyd, C. Ramanathan, and P. Cappellaro, Emergent prethermalization signatures in out-of-time ordered correlations, *Phys. Rev. Lett.* **123**, 090605 (2019).
- [42] P. Reimann and L. Dabelow, Typicality of prethermalization, *Phys. Rev. Lett.* **122**, 080603 (2019).
- [43] P. Peng, C. Yin, X. Huang, C. Ramanathan, and P. Cappellaro, Floquet prethermalization in dipolar spin chains, *Nat. Phys.* **17**, 444 (2021).
- [44] S. Birnkammer, A. Bastianello, and M. Knap, Prethermalization in one-dimensional quantum many-body systems with confinement, *Nat. Commun.* **13**, 7663 (2022).
- [45] M. Alexander and M. Kollar, Photoinduced prethermalization phenomena in correlated metals, *Phys. Status Solidi B* **259**, 2100280 (2022).
- [46] H.-K. Jin, J. Knolle, and M. Knap, Fractionalized prethermalization in a driven quantum spin liquid, *Phys. Rev. Lett.* **130**, 226701 (2023).
- [47] Y. Le, Y. Zhang, S. Gopalakrishnan, M. Rigol, and D. S. Weiss, Direct observation of hydrodynamization and local prethermalization, *Nature (London)* **618**, 494 (2023).
- [48] M. Ueda, Quantum equilibration, thermalization and prethermalization in ultracold atoms, *Nat. Rev. Phys.* **2**, 669 (2020).
- [49] T. Mori, T. N. Ikeda, E. Kaminishi, and M. Ueda, Thermalization and prethermalization in isolated quantum systems: A theoretical overview, *J. Phys. B* **51**, 112001 (2018).
- [50] K. Mallayya, M. Rigol, and W. De Roeck, Prethermalization and thermalization in isolated quantum systems, *Phys. Rev. X* **9**, 021027 (2019).

- [51] K. Mallayya and M. Rigol, Quantum quenches and relaxation dynamics in the thermodynamic limit, *Phys. Rev. Lett.* **120**, 070603 (2018).
- [52] F. Queisser and R. Schützhold, Boltzmann relaxation dynamics in the strongly interacting Fermi-Hubbard model, *Phys. Rev. A* **100**, 053617 (2019).
- [53] F. Queisser, S. Schreiber, P. Kratzer, and R. Schützhold, Boltzmann relaxation dynamics of strongly interacting spinless fermions on a lattice, *Phys. Rev. B* **100**, 245110 (2019).
- [54] F. Queisser, G. Schaller, and R. Schützhold, Attraction versus repulsion between doublons or holons in Mott-Hubbard systems, *Int. J. Theor. Phys.* **62**, 239 (2023).
- [55] P. Navez and R. Schützhold, Emergence of coherence in the Mott-insulator–superfluid quench of the Bose-Hubbard model, *Phys. Rev. A* **82**, 063603 (2010).
- [56] F. H. L. Essler, H. Frahm, F. Göhmann, A. Klümper, and V. E. Korepin, *The One-Dimensional Hubbard Model* (Cambridge University Press, Cambridge, 2005).
- [57] A. Georges and G. Kotliar, Hubbard model in infinite dimensions, *Phys. Rev. B* **45**, 6479 (1992).
- [58] F. Queisser, K. V. Krutitsky, P. Navez, and R. Schützhold, Equilibration and prethermalization in the Bose-Hubbard and Fermi-Hubbard models, *Phys. Rev. A* **89**, 033616 (2014).
- [59] F. Queisser and R. Schützhold, Hierarchy of double-time correlations, *J. Stat. Mech.* (2023) 053101.
- [60] R. Eder and K. W. Becker, Coherent motion of a hole in a two-dimensional quantum antiferromagnet, *Z. Phys. B* **78**, 219 (1990).
- [61] A. Belkasri and J. L. Richard, Motion of a single hole in a disordered magnetic background, *Phys. Lett. A* **197**, 353 (1995).
- [62] M. Vojta and K. W. Becker, Hole motion in an arbitrary spin background: Beyond the minimal spin-polaron approximation, *Phys. Rev. B* **57**, 3099 (1998).
- [63] P. Bleicker, D.-B. Hering, and G. S. Uhrig, Charge dynamics in magnetically disordered Mott insulators, *Phys. Rev. B* **105**, 085121 (2022).
- [64] Y. F. Kung, E. A. Nowadnick, C. J. Jia, S. Johnston, B. Moritz, R. T. Scalettar, and T. P. Devereaux, Doping evolution of spin and charge excitations in the Hubbard model, *Phys. Rev. B* **92**, 195108 (2015).
- [65] T. Herrmann and W. Nolting, Magnetism in the single-band Hubbard model, *J. Magn. Magn. Mater.* **170**, 253 (1997).
- [66] A. Picano, J. Li, and M. Eckstein, Quantum Boltzmann equation for strongly correlated electrons, *Phys. Rev. B* **104**, 085108 (2021).
- [67] A. Georges, G. Kotliar, W. Krauth, and M. J. Rozenberg, Dynamical mean-field theory of strongly correlated fermion systems and the limit of infinite dimensions, *Rev. Mod. Phys.* **68**, 13 (1996).
- [68] M. Eckstein, M. Kollar, and P. Werner, Thermalization after an interaction quench in the Hubbard model, *Phys. Rev. Lett.* **103**, 056403 (2009).
- [69] M. Eckstein, M. Kollar, and P. Werner, Interaction quench in the Hubbard model: Relaxation of the spectral function and the optical conductivity, *Phys. Rev. B* **81**, 115131 (2010).
- [70] M. Eckstein and P. Werner, Nonequilibrium dynamical mean-field calculations based on the noncrossing approximation and its generalizations, *Phys. Rev. B* **82**, 115115 (2010).
- [71] N. Tsuji, P. Barmettler, H. Aoki, and P. Werner, Nonequilibrium dynamical cluster theory, *Phys. Rev. B* **90**, 075117 (2014).